University of New Mexico

Doctoral Thesis

Advanced Methods in Stochastic Collocation for Polynomial Chaos in RAVEN

Author:
Paul W. Talbot

Supervisor:
Dr. Anil K. Prinja

Submitted in partial fulfillment of the requirements
for the degree of Doctor of Philosophy in Engineering

in the

Department of Nuclear Engineering

July 2016

Abstract

As experiment complexity in fields such as nuclear engineering continues to increase, so does the demand for robust computational methods to simulate them. In many simulations, input design parameters as well as intrinsic experiment properties are sources of input uncertainty. Often, small perturbations in uncertain parameters have significant impact on the experiment outcome. For instance, when considering nuclear fuel performance, small changes in the fuel thermal conductivity can greatly affect the maximum stress on the surrounding cladding. The difficulty of quantifying input uncertainty impact in such systems has grown with the complexity of the numerical models. Traditionally, uncertainty quantification has been approached using random sampling methods like Monte Carlo. For some models, the input parametric space and corresponding quantity-of-interest output space is sufficiently explored with a few low-cost computational calculations. For other models, it is computationally costly to obtain a good understanding of the output space.

To combat the costliness of random sampling, this research explores the possibilities of advanced methods in stochastic collocation for generalized polynomial chaos (SCgPC) as an alternative to traditional uncertainty quantification techniques such as Monte Carlo (MC) and Latin Hypercube sampling (LHS) methods. In this proposal we explore the behavior of traditional SCgPC construction strategies, as well as truncated polynomial spaces using total degree (TD) and hyperbolic cross (HC) construction strategies. We also consider applying anisotropy to the polynomial space, and analyze methods whereby the level of anisotropy can be approximated. We review and develop potential adaptive polynomial construction strategies. Finally, we add high-dimension model reduction (HDMR) expansions, using SCgPC representations for the constituent terms, and consider adaptive methods to construct them. We analyze these methods on a series of models of increasing complexity. We primarily use analytic methods of various means, and finally demonstrate on an engineering-scale neutron transport problem. For this analysis, we demonstrate the application of the algorithms discussed above in `raven`, a production-level uncertainty quantification framework.

Finally, we propose additional work in enhancing the current implementations of SCgPC and HDMR.

Contents

List of Figures

List of Tables

Chapter 1

Introduction

In simulation modeling, we attempt to capture the behavior of a physical system by describing it in a series of equations, often partial differential equations. These equations may be time-dependent, and capture physics of interest for understanding the system. A *solver* is then written that can solve the series of equations and determine quantities of interest (QoI). A traditional solver accepts a set of inputs and produces a set of single-valued outputs. For instance, a solver might solve equations related to the attenuation of a beam of photons through a material, and the QoI might be the strength of the beam exiting the material. A single run of the solver usually results in a single value, or realization, of the quantity of interest.

This single realization might be misleading, however. In most systems there is some degree of uncertainty in the input parameters to the solver. Some of these uncertainties may be epistemic, or systematic uncertainty originating with inexact measurements or measurable unknowns. Other uncertainties might be aleatoric, intrinsic uncertainty in the system itself, such as probabilistic interactions or random motion. Taken together, the input parameter uncertainties exist within a multidimensional probabilistic space. While some points in that space may be more likely than others, the possible range of values for the QoI is only understood when the uncertain input space is considered as a whole. We note here that while it is possible that some of the input parameters are correlated in their probabilistic distribution, it is also possible to decouple them into uncorrelated variables. Throughout this work we will assume the input parameters are uncorrelated.

One traditional method for exploring the uncertain input space is through random sampling, such as in analog Monte Carlo sampling. In this method, a point in the input space is chosen at random based on probability. This point represents values for the input parameters to the solver. The solver is executed with these inputs, and the QoIs

are collected. Then, another point in the input space is chosen at random. This process continues until the properties of the QoIs, or *response*, are well understood.

There are some beneficial properties to random sampling approaches like Monte Carlo. Significantly, they are unintrusive: there is no need to modify the solver in order to use these methods. This allows a framework of algorithms to be developed which know only the input space and QoI of a solver, but need no further knowledge about its operation. Unintrusive methods are desirable because the uncertainty quantification algorithms can be developed and maintained separately from the solver.

Monte Carlo and similar sampling strategies are relatively slow to converge on the response surface. For example, with Monte Carlo sampling, in order to reduce the standard error of the mean of the response by a factor of two, it is necessary to take at least four times as many samples. If a solver is sufficiently computationally inexpensive, running additional solutions is not a large concern; however, for lengthy and expensive solvers, it may not be practical to obtain sufficient realizations to obtain a clear response.

In this work, we will assume solvers are computationally expensive, requiring many hours per solve, and that computational resource availability requires as few solves as possible. As such, we consider several methodologies for quantifying the uncertainty in expensive solver calculations. In order to demonstrate clearly the function of these methods, we apply them first on several simpler problems, such as polynomial evaluations and analytic attenuation. These models have a high degree of regularity, and their analyticity provides for straightforward benchmarking. Through gradual increasing complexity, we investigate the behavior of the UQ methods.

Finally, we apply the methods to an engineering-scale solver that models the neutronics and performance of nuclear fuel. This will demonstrate the practical application of the uncertainty quantification methods, where the regularity and other properties of the model are not well understood.

The first uncertainty quantification method we consider is traditional analog Monte Carlo (MC) analysis, wherein random sampling of the input space generates a view of the response. MC is used as a benchmark methodology; if other methods converge on moments of the quantities of interest more quickly and consistently than MC, we consider them "better" for our purposes.

The second method we consider is stochastic collocation for generalized polynomial chaos (SCgPC)[11, 22–24], whereby deterministic collocation points are used to develop a polynomial-interpolated reduced-order model of the response as a function of the inputs. This method algorithmically expands the solver as the sum of orthogonal multi-dimensional polynomials with scalar coefficients. The scalar coefficients are obtained by

numerical integration using multidimensional collocation (quadrature) points. The chief distinction between SCgPC and Monte Carlo methods is that SCgPC is deterministic, in that the realizations required from the solver are predetermined instead of randomly sampled. There are two major classes of deterministic uncertainty quantification methods: intrusive and unintrusive. Like Monte Carlo, SCgPC is unintrusive and performs well without any need to access the operation of the solver. This behavior is desirable for construction black-box approach algorithms for uncertainty quantification. Other intrusive methods such as stochastic Galerkin exist [5], but require solver modification to operate. This makes them solver-dependent and undesirable for an independent uncertainty quantification framework.

The other methods we present here expand on SCgPC. First, we introduce non-tensor-product methods for determining the set of polynomial bases to use in the expansion. Because a tensor product grows exponentially with increasing cardinality of the input space, we combat this curse of dimensionality using the alternative polynomial set construction methods[13]. These bases will then be used to construct Smolyak-like sparse grids [14] to provide collocation points that in turn calculate the coefficients in the polynomial expansion. Second, we consider anisotropic sparse grids, allowing higher-order polynomials for particular input parameters. We also consider methods for obtaining weights that determine the level of anisotropic preference to give parameters, and explore the effects of a variety of anisotropic choices.

The second method group we consider is high-dimension model representation (HDMR), which correlates with Sobol decomposition [20]. This method is useful both for developing sensitivities of the quantity of interest to subsets of the input space, as well as constructing a reduced-order model itself. We demonstrate the strength of HDMR as a method to inform anisotropic sensitivity weights for SCgPC.

Finally, we consider adaptive algorithms to construct both SCgPC and HDMR expansions using second-moment convergence criteria. We analyze these for potential efficiencies and shortcomings. We also propose future work to further improve the adaptive methods.

We implement all these methods in Idaho National Laboratory's `raven`[9] uncertainty quantification framework. `raven` is a Python-written framework that non-intrusively provides tools for analysts to quantify the uncertainty in their simulations with minimal development. To demonstrate the application of the method developed, we use a complex non-linear multiphysics system solver simulating the operation of a fuel pin within a nuclear reactor core, including both neutronics and fuel performance physics kernals. For this solver, we use the coupled `rattleSNake`[10] and `bison` [6, 8] production codes. Both of these codes are developed and maintained within the `moose`[7] environment. The

multiphysics nonlinear system provides a challenge with unknown response properties for the uncertainty quantification methods discussed in this proposal.

The remainder of this work will proceed as follows:

- Chapter 2: We describe the analytic test problems and engineering-scale problem solved by the simulations we will be running, along with their properties and inferences about the algorithms developed. We discuss potential approaches to model solving and applications of the models.
- Chapter 3: We describe methods for uncertainty quantification, including Monte Carlo (MC), stochastic collocation for generalized Polynomial Chaos (SCgPC), and high-dimension model reduction (HDMR). We additionally describe adaptive methods for SCgPC and HDMR.
- Chapter 4: We analyze results obtained for the various UQ methods on analytic models, and contrast them with traditional Monte Carlo convergence on statistical moments.
- Chapter 5: We perform analysis on the engineering-scale multiphysics coupled problem, and analyze results.
- Chapter 6: We draw conclusions from the evaluations performed, and offer some suggestions for applicability as well as future development for the UQ methods demonstrated.

Chapter 2

Models

2.1 Introduction to Models

In this section we present the models used in demonstrating the uncertainty quantification (UQ) methods in this work. We use the term *model* to describe any code with uncertain inputs and a set of at least one response quantity of interest. We include a variety of models with the intent to demonstrate the strengths and weaknesses of each UQ method.

Firstly, we include several analytic models. These are models who have an exact, derivable value for statistical moments or sensitivities. They are simpler in mechanics than full engineering-scale problems, and offer a way to benchmark the performance of the UQ methods.

Secondly, we include an engineering-scale multiphysics application. There are no analytic response values in this model, only a nominal case with no uncertainty included in the input space. Demonstration of the performance of UQ methods on this model will highlight the practical application of each method.

We describe each model in turn. Throughout the models, we will describe them using the syntax

$$u(Y) = Q, \tag{2.1}$$

where $u(Y)$ is the model as a function of N uncertain inputs $Y = (y_1, \ldots, y_N)$ and Q is a single-valued response quantity of interest.

2.2 Tensor Monomials

The simplest model we make use of is a first-order tensor polynomial (tensor monomial) combination **??**. The mathematical expression is

$$u(Y) = \prod_{n=1}^{N} (y_n + 1). \tag{2.2}$$

For example, for $N = 3$ we have

$$u(Y) = y_1 y_2 y_3 + y_1 y_2 + y_1 y_3 + y_2 y_3 + y_1 + y_2 + y_3 + 1. \tag{2.3}$$

For this model we distribute the uncertain inputs in several ways: uniformly on [-1,1], uniformly on [0,1], and normally on $[\mu, \sigma]$. A summary of analytic statistics is given in Table 2.1.

Distribution	Mean	Variance
$\mathcal{U}[-1,1]$	1	$\left(\frac{4}{3}\right)^N - 1$
$\mathcal{U}[0,1]$	$\left(\frac{3}{4}\right)^N$	$\left(\frac{7}{3}\right)^N - \left(\frac{3}{4}\right)^{2N}$
$\mathcal{N}[\mu,\sigma]$	$\prod_{n=1}^{N}(\mu_{y_n}+1)$	$\prod_{n=1}^{N}[(\mu_{y_n}+1)^2+\sigma_{y_n}^2] - \prod_{n=1}^{N}(\mu_{y_n}+1)^2$

TABLE 2.1: Analytic Expressions for Tensor Monomial Case

2.3 Sudret Polynomial

The polynomial used by Sudret in his work [30] is another tensor-like polynomial, and is a test case traditionally used to identify convergence on sensitivity parameters. The mathematical expression is

$$u(Y) = \frac{1}{2^N} \prod_{n=1}^{N} (3y_n^2 + 1). \tag{2.4}$$

The variables are distributed uniformly on [0,1]. The statistical moments and sensitivities are given in Table 2.2, where $\mathcal{S}_n$ is the global Sobol sensitivity of $u(Y)$ to perturbations in y_n.

Statistic	Expression
Mean	1
Variance	$\left(\frac{6}{5}\right)^N - 1$
$\mathcal{S}_n$	$\frac{5^{-n}}{(6/5)^N - 1}$

TABLE 2.2: Analytic Expressions for Sudret Case

2.4 Attenuation

This model represents an idealized single-dimension system where an beam of particles impinges on a purely-absorbing material with total scaled length of 1. The response of interest is the fraction of particles exiting the opposite side of the material. The material is divided into N segments, each of which has a distinct uncertain absorption cross section y_n. The solution takes the form

$$u(Y) = \prod_{n=1}^{N} \exp(-y_n/N). \tag{2.5}$$

Because negative cross sections have dubious physical meaning, we restrict the distribution cases to uniform on [0,1] as well as normally-distributed on $[\mu, \sigma]$. A summary of analytic statistics is given in Table 2.3.

Distribution	Mean	Variance
$\mathcal{U}[0,1]$	$\left[N\left(1-e^{-1/N}\right)\right]^N$	$\left[\frac{N}{2}\left(1-e^{-2/N}\right)\right]^N - \left[N\left(1-e^{-1/N}\right)\right]^{2N}$
$\mathcal{N}[\mu,\sigma]$	$\prod_{n=1}^{N} \exp\left[\frac{\sigma_{y_n}^2}{2N^2} - \frac{\mu_{y_n}}{N}\right]$	$\prod_{n=1}^{N} \exp\left[\frac{2\sigma_{y_n}^2}{N^2} - \frac{2\mu_{y_n}}{N}\right]$

TABLE 2.3: Analytic Expressions for Attenuation Case

This model has some interesting properties to demonstrate performance of polynomial-based UQ methods. First, because the solution is a product of exponential functions, it cannot be exactly represented by a finite number of polynomials. Second, the Taylor development of the exponential function includes all increasing polynomial orders. The product of several exponential functions is effectively a tensor combination of polynomials for each dimension.

2.5 Gaussian Peak

Similar to the attenuation model, the Gaussian peak [31] instead uses square arguments to the exponential function. A tuning parameter a can be used to change the peakedness of the function. Increased peakedness leads to more difficult polynomial representation. A location parameter μ can be used to change the location of the peak. The mathematical expression is

$$u(Y) = \exp\left(-\sum_{n=1}^{N} a^2(y_n - \mu)^2\right). \tag{2.6}$$

We allow each y_n to vary uniformly on [0,1]. A summary of analytic statistics is given in Table 2.4.

Statistic	Expression
Mean	$\left(\frac{\sqrt{\pi}}{2a}(\operatorname{erf}(a\mu)+\operatorname{erf}(a-a\mu))\right)^N$
Variance	$\left(\frac{\sqrt{\pi/2}}{2a}\left(\operatorname{erf}(a\mu\sqrt{2})-\operatorname{erf}(a\sqrt{2}(1-\mu))\right)\right)^N-\left(\frac{\sqrt{\pi}}{2a}(\operatorname{erf}(a\mu)+\operatorname{erf}(a-a\mu))\right)^{2N}$

TABLE 2.4: Analytic Expressions for Gaussian Peak Case

This case offers particular challenge because of its Taylor development, which only includes even powers of the uncertain parameters. This suggests added difficulty in successive representation, especially for an adaptive algorithm.

2.6 Ishigami Function

The Ishigami function [32] is a commonly-used function in performing sensitivity analysis. It is given by

$$u(Y) = \sin y_1 + a\sin^2 y_2 + by_3^4 \sin(y_1). \tag{2.7}$$

In our case, we will use $a = 7$ and $b = 0.1$ as in [33]. In particular interest for this model are its strong nonlinearity and lack of independence for y_3, as it only appears in conjunction with y_1. The analytic statistics of interest for this model are in Table 2.5, where D_n is the partial variance contributed by y_n and Sobol sensitivities $\mathcal{S}_n$ are obtained by dividing D_n by the total variance.

Statistic	Expression	Approx. Value
Mean	$\frac{7}{2}$	3.5
Variance	$\frac{a^2}{8}+\frac{b\pi^4}{5}+\frac{b^2\pi^8}{18}+\frac{1}{2}$	13.84459
D_1	$\frac{b\pi^4}{5}+\frac{b^2\pi^8}{50}+\frac{1}{2}$	4.34589
D_2	$\frac{a^2}{8}$	6.125
$D_{1,3}$	$\frac{8b^2\pi^8}{225}$	3.3737
$D_3, D_{1,2}, D_{2,3}, D_{1,2,3}$	0	0

TABLE 2.5: Analytic Expressions for Ishigami Case

2.7 Sobol G-Function

2.8 Anisotropic Polynomial

2.9 Pin Cell

This model is a coupled multiphysics engineering-scale model. It simulates fuel behavior through the depletion of fissile material in a single two-dimensional slice of a fuel rod. The problem domain contains the fuel, gap, clad, and moderator, and represents a symmetric quarter pin. The depletion steps are carried out through a year-long burn cycle. The coupled multiphysics are neutronics, handled by `rattleSNake`, and fuel performance, handled by `bison`.

The mesh is shown in Fig. **??**. TODO BETTER FIGURE. The mesh contains 20 bands of fuel blocks, the gap, the clad, and the moderator. TODO Use colors to describe locations. TODO dimensions.

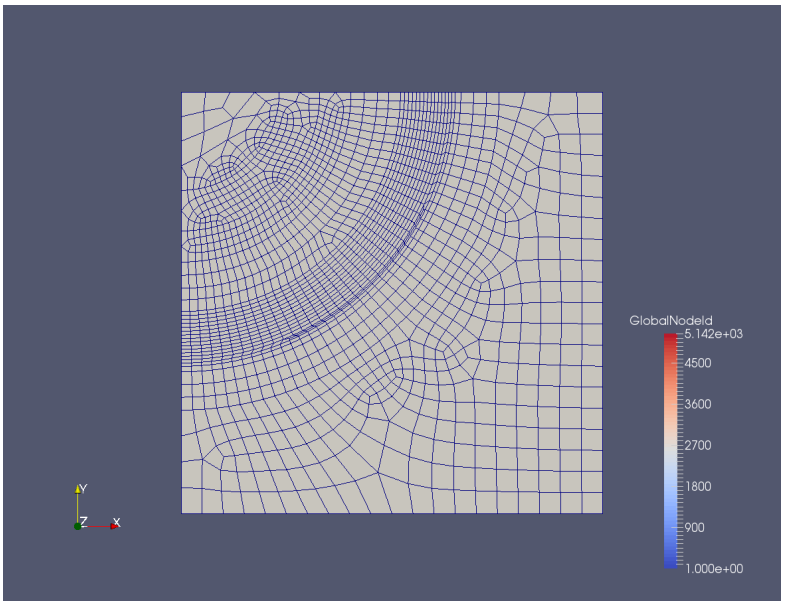

The neutronics is calculated using 8 energy groups and takes as uncertain inputs 671 material cross sections, including fission, capture, scattering, and neutron multiplication factor Each cross section is perturbed by 10% of its original value, distributed normally. The scattering cross sections for each material in each group are not perturbed individually; rather, a scattering scaling factor for each group is determined, and the scattering cross sections are all scaled by that factor. The fission and capture cross sections are perturbed individually. The critical output of the neutronics calculation is power shapes for use in the fuel performance code, as well as the k-eigenvalue for the rod.

The fuel performance code models mechanics such as heat conduction in the fuel, clad, and gap, clad stresses, grain radius growth, and fuel expansion through the depletion steps of the fuel. The code takes power shapes from the neutronics code as input and produces several key characteristics, such as peak clad temperature, maximum fuel centerline temperature, and maximum clad stress.

The uncertain input space is highly correlated, so a Karhunen-Loeve (KL) component analysis is performed as the first step in a two-part reduction [28]. The covariance matrix is obtained via cross section construction in `scale`[29] using random sampling. Table 2.6 gives the first several eigenvalues in the KL expansion. Surrogate (or *latent*) dimensions identified by the KL expansion will be used as input variables for demonstration of the various UQ methods.

Index	Eigenvalue
1	0.974489839965
2	0.0183147250746
3	0.00271597405394
4	0.00260939137165
5	0.000486257522596
6	0.000431957645049
7	0.000253683187786
8	0.000228044411204
9	0.000124030638175
10	7.14328494102e-05
11	6.30833696364e-05
12	3.87071149672e-05
13	3.51066363934e-05
14	2.48699823434e-05
15	1.98915286765e-05
16	1.35985387253e-05
17	1.128896325e-05
18	9.59426898684e-06
19	8.11612567548e-06
20	7.16508951777e-06
21	6.53366817241e-06
22	4.50006575957e-06
23	4.19287192651e-06
24	3.7671309151e-06
25	2.61683536224e-06
26	2.22099981728e-06
27	1.6360971709e-06
28	1.13245742809e-06
29	9.92282537141e-07

TABLE 2.6: KL Expansion Eigenvalues for Pin Cell Problem

Chapter 3

Methods

3.1 Introduction

In this chapter we describe various common uncertainty quantification methods and their applications. We begin by discussing the principles of input spaces and responses, and define terminology used in this work. Next we discuss uncertainty quantification at a high level, and describe several common uncertainty quantification tools. Finally, we explore generalized polynomial chaos expansion, stochastic collocation, and high-density model reduction as advanced uncertainty quantification techniques.

Many simulation models are algorithms constructed to solve partial differential equations, often in two or three dimensions and possibly time. The inputs to these models include boundary conditions, material properties, tuning parameters, and so forth. The outputs are quantities of interest, either data fields or scalar values. The outputs are used to inform decision-making processes. In general, we allow $u(Y)$ to be the model u as a function of the input space $Y = (y_1, \ldots, y_n, \ldots, y_N)$ where y_n is a single input parameter to the model, n is an index spanning the number of inputs, and N is the total number of inputs. We signify the output response quantity as Q, and assume it to be a scalar integrated quantity. Our generic model takes the form

$$u(Y) = Q. \tag{3.1}$$

Essential to using simulation models is understanding the possibility of important uncertainties existing in the inputs. These could be aleatoric uncertainties due to intrinsic randomness in the inputs, or epistemic uncertainties due to model imperfections or lack of knowledge. Each of these uncertainties has some distribution defining the likelihood

of an input to have a particular value. These distributions might be assumed or constructed from experiment; for our work, we will assume given distributions are accurate. The input likelihood distribution is the probability distribution function (PDF) $\rho_n(y_n)$. We require

$$\int_a^b \rho_n(y_n) d\ y_n = 1, \tag{3.2}$$

where a and b are the minimum and maximum values y_n can take (possibly infinite).

When there are more than one uncertain input, the combination of distributions for these inputs span an uncertainty space Ω. TODO make sure this terminology is right. The dimensionality of Ω is N, the number of uncertain input variables. The probability of any point in the input space occurring is given by the join-probability distribution $\rho(Y)$, still enforcing

$$\int_{a_1}^{b_1} \cdots \int_{a_N}^{b_N} \rho(Y) dy_1 \cdots dy_N = 1. \tag{3.3}$$

. For clarity, we define multidimensional integral operator

$$\int_\Omega (\cdot) dY \equiv \int_{a_1}^{b_1} \cdots \int_{a_N}^{b_N} (\cdot) dy_1 \cdots dy_N, \tag{3.4}$$

so that Eq. 3.3 can be written

$$\int_\Omega \rho(Y) dY = 1. \tag{3.5}$$

We note the possibility that multiple inputs may be correlated with each other. When inputs are not independent, the joint probability distribution is not the product of each individual probability distribution distribution. Using principle component analysis (sometimes known as Karhunen-Loeve expansion [**?**]), however, a surrogate orthogonal input space can be constructed. As a result, we only consider independent variables in this work.

3.2 Uncertainty Quantification

The purpose of uncertainty quantification is to propagate the uncertainties present in the input space of a problem through the model and comprehend their effects on the output responses. Often response uncertainty is quantified in terms of moments. Second-order uncertainty quantification seeks for the mean and variance of the perturbed response. In general, the mean of a model is the first moment,

$$\text{mean} = \mathbb{E}[u(Y)] = \int_\Omega \rho(Y) u(Y) dY, \tag{3.6}$$

and the variance is the second moment less the square of the first,

$$\text{variance} = \mathbb{E}[u(Y)^2] = \int_\Omega \rho(Y) u(Y)^2 dY, \tag{3.7}$$

Another use for uncertainty quantification is understanding the sensitivity of the output responses to the uncertain inputs; that is, determining how responses change as a function of changes in the input space. At the most primitive level, linear sensitivity of a response mean to an input is the derivative of the response with respect to the input. Sensitivities can be both local to a region in the input space as well as global to the entire problem.

There are several common tools used for uncertainty quantification when analytic analysis is not possible. These include stochastic methods such as Monte Carlo sampling, deterministic methods such as Grid sampling, and mixed methods such as Latin Hypercube sampling.

3.2.1 Monte Carlo

The Monte Carlo method [**?**] has been used formally since the 1930s as a tool to explore possible outcomes in uncertain models. Nuclear physicist Enrico Fermi used the method in his work with neutron moderation in Rome [**?**]. In its simplest form, Monte Carlo involves randomly picking realizations from a set of possibilities, then statistically collecting the results. In uncertainty quantification, Monte Carlo can be used to sample points in the input space based on the joint probability distribution. The collection of points is analyzed to determine the moments of the response.

The mean of a response is determined using

Chapter 4

Analytic Results

4.1 Introduction

In this chapter we present results obtained using stochastic collocation for generalized polynomial chaos expansions (SCgPC) and high-dimension model reduction (HDMR) uncertainty quantification methods. In each case we also include Monte Carlo as a comparison benchmark.

Our primary objective in expanding the usability of collocation-based methods is to reduce the number of computational model solves necessary to obtain reasonable second-order statistics for the model. For each analytic model described in Chapter 3, we present value figures and convergence figures.

Value figures show the values of the mean or standard deviation obtained, along with the benchmark analytic value as a dotted line. The Monte Carlo samples are taken at a few select points. Error bars are provided for the Monte Carlo method and are estimated using the population variance,

$$\epsilon_{95} = \frac{1.96\bar{\sigma}_N}{\sqrt{N}}, \tag{4.1}$$

$$\bar{\sigma}_N^2 = \frac{N}{N-1}\sigma_N^2 = \frac{N}{N-1}\left(\frac{1}{N}\sum_{i=1}^{M} u(Y_i)^2 - \bar{u}(Y)_N^2\right), \tag{4.2}$$

where Y_i are a set of M independent identically-distributed realizations taken from the input space. These errorbars estimate where the value of the statistic is with a probability near 0.95. The estimate of this error improves as additional samples are taken.

Convergence figures are log-log error graphs with the number of computational solves on the x-axis and error with the analytical solution on the y-axis. The distinct lines

demonstrate series of results obtained for each UQ method. Each series obtains additional values by increasing the refinement of the method. For Monte Carlo, additional samples are added. For static SCgPC, higher-order polynomials are used in the representative expansion. For adaptive methods, additional solves are allowed to adaptively include additional polynomials and/or dimension subsets.

The measure of success for a method is less dependent on the absolute value of the error shown. Instead, the rate of convergence as refinement increases determines the desirability of the method for that model. We expect the rate of convergence to depend on two factors: the dimensionality of the uncertain space for the model, and the continuity of the response measured. We consider the convergence of both the mean and the standard deviation for each model.

The series considered include analog Monte Carlo (mc), Tensor Product polynomial expansion construction method (tp), Total Degree polynomial expansion construction method (td), Hyperbolic Cross polynomial expansion construction method (hc), adaptive sparse grid collocation for generalized polynomial chaos expansion (adaptSC), and adaptive HDMR or adaptive Sobol decomposition (adaptSobol).

We additionally note that results from `raven` computations were written to file using 10 digits of accuracy. As a result, any apparent convergence past this level of accuracy is coincidental or the result of machine-exact values, and we consider a relative difference of 10^{-10} to be converged.

4.2 Tensor Monomials

This model is described in section 2.2. As this polynomial contains only combinations of first-order polynomials, we expect the Tensor Product index set construction method (TP) to be very efficient in absolute error magnitude. Because the model has infinite continuity, we expect all collocation-based methods to be quite efficient. The values and errors of the mean and standard deviation are given in Figures 4.5 through 4.8 for 5 uncertain inputs, and the same for 10 dimensions is given in Figures 4.9 through 4.12. Note that TP exactly reproduces the original model with expansion order 1, so no convergence is observed past the initial sampling point.

4.2.1 3 Inputs

The strength of collocation methods is clear for this small-dimensionality problem of three uncertain inputs. The convergence on the mean and standard deviation is swift

for all the methods. Both adaptive methods converge at nearly identical rates; this is not surprising, as for small dimension problems the adaptive search follows a very similar path.

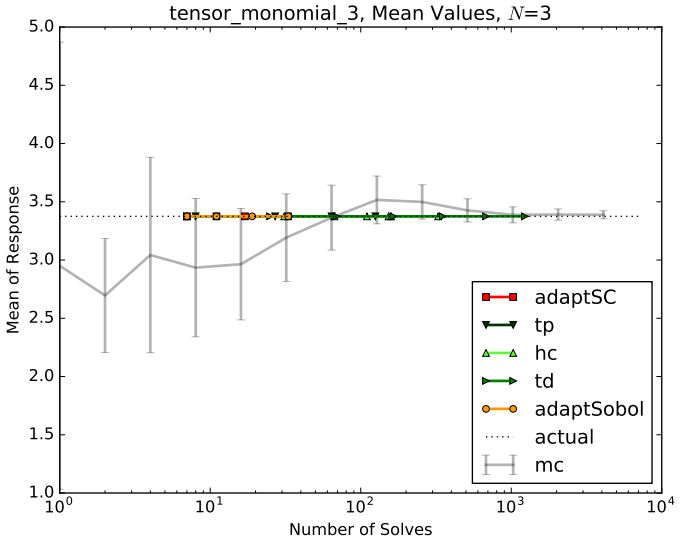

FIGURE 4.1: Tensor Monomial, $N = 3$, Mean Values

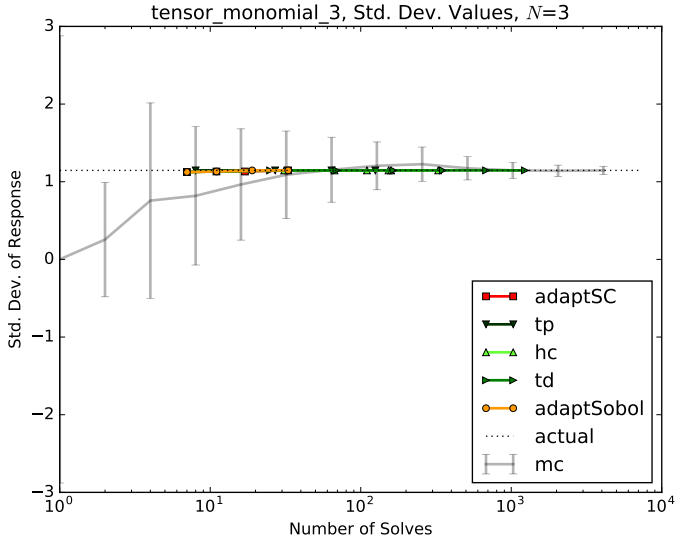

FIGURE 4.2: Tensor Monomial, $N = 3$, Std. Dev. Values

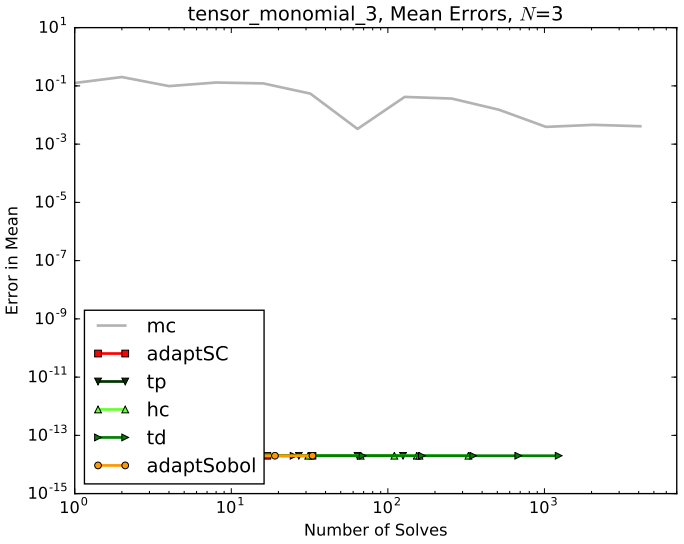

FIGURE 4.3: Tensor Monomial, $N = 3$, Mean Convergence

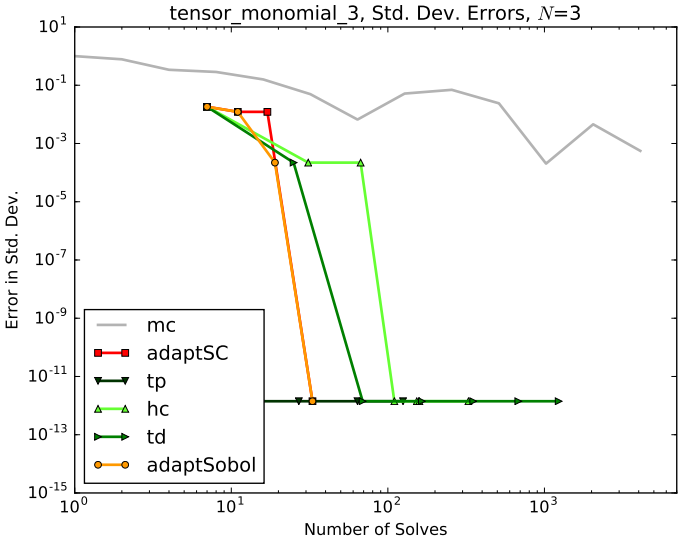

FIGURE 4.4: Tensor Monomial, $N = 3$, Std. Dev. Convergence

4.2.2 5 Inputs

While the convergence on the mean is still direct for the five-dimensional input problem, we begin to see degradation in the convergence of collocation-based methods. Total Degree outperforms adaptive methods, as the search algorithms struggle to find the optimal tensors of low-order polynomials required. Hyperbolic Cross is outperformed by Total Degree, as expected for a problem with this level of regularity.

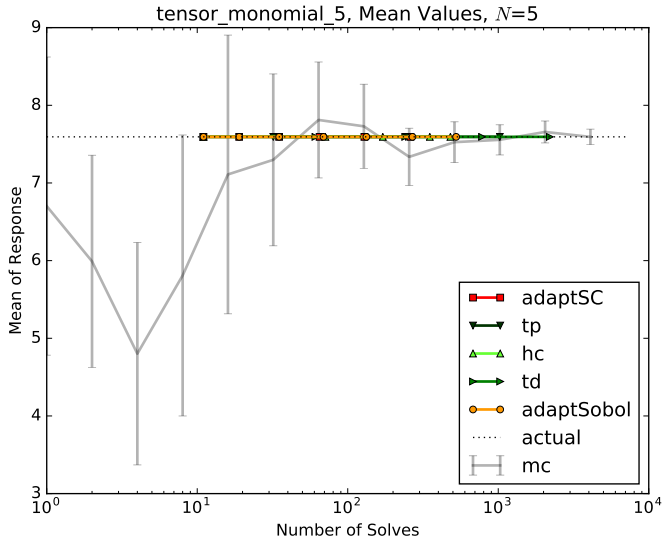

FIGURE 4.5: Tensor Monomial, $N = 5$, Mean Values

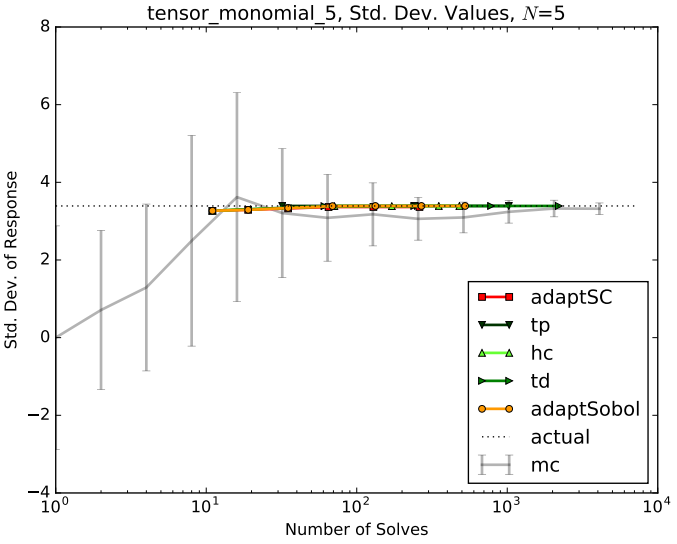

FIGURE 4.6: Tensor Monomial, $N = 5$, Std. Dev. Values

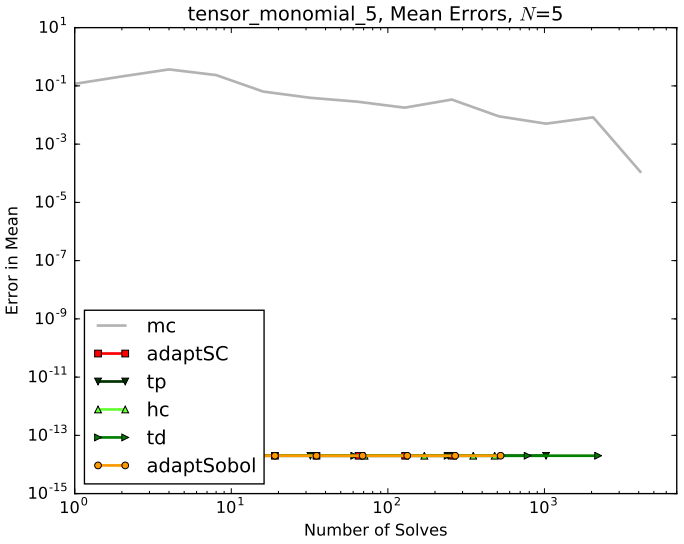

FIGURE 4.7: Tensor Monomial, $N = 5$, Mean Convergence

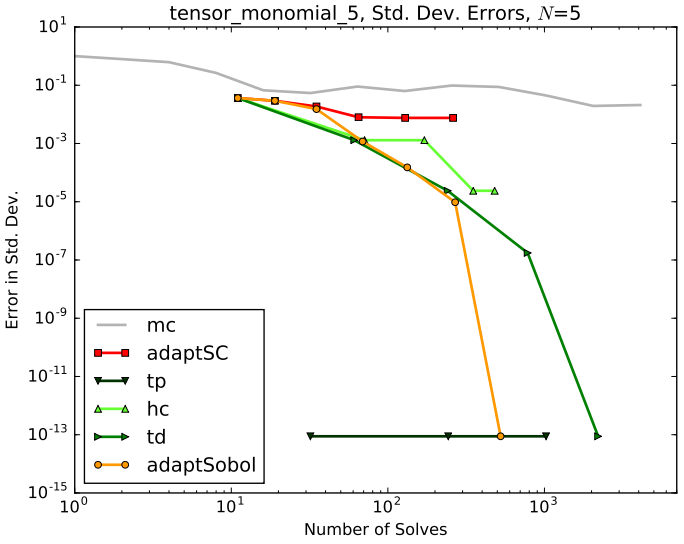

FIGURE 4.8: Tensor Monomial, $N = 5$, Std. Dev. Convergence

4.2.3 10 Inputs

As we increase to ten inputs, we see significant degradation of all the collocation methods in converging on the standard deviation. While it appears there is exponential convergence, the curvature is quite large, and little better than linear convergence is observed for up to 1000 computational solves. One reason the adaptive methods do not perform more admirably for this case is the equal-weight importance of all the input terms as well as the polynomial terms; the high-dimensional space takes considerable numbers of runs

to explore thoroughly, and this model contains some of the most difficult polynomials to find adaptively: those including all of the inputs.

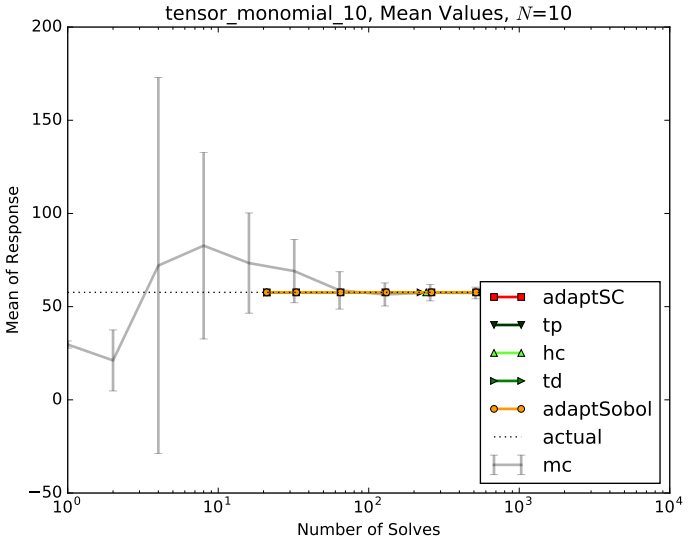

FIGURE 4.9: Tensor Monomial, $N = 10$, Mean Values

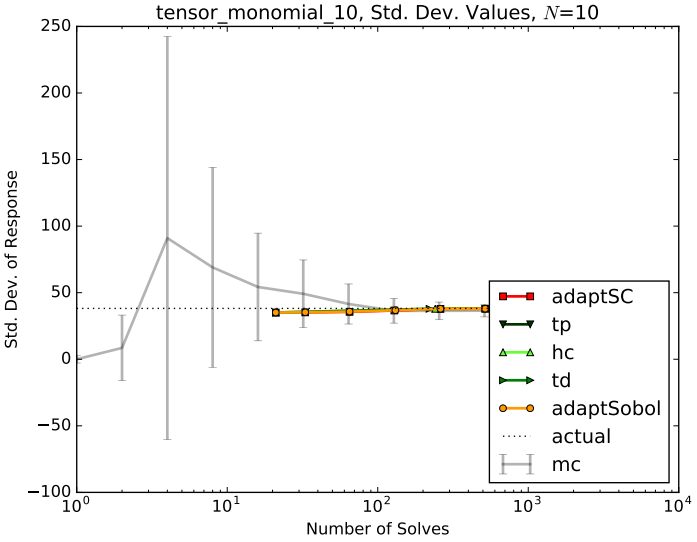

FIGURE 4.10: Tensor Monomial, $N = 10$, Std. Dev. Values

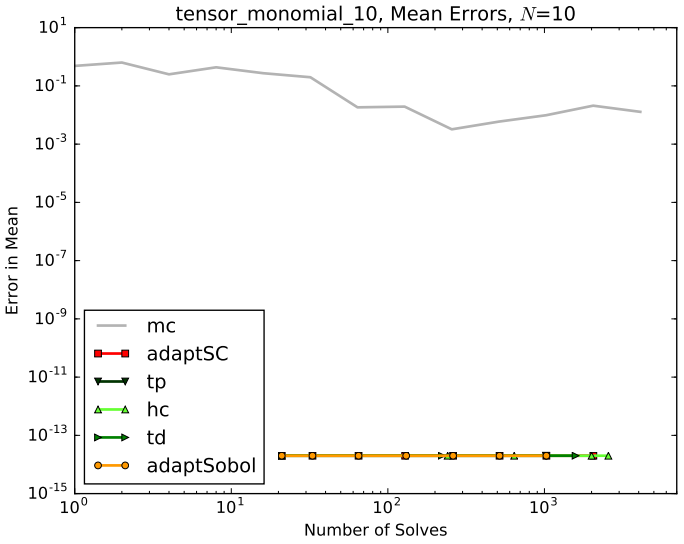

FIGURE 4.11: Tensor Monomial, $N = 10$, Mean Convergence

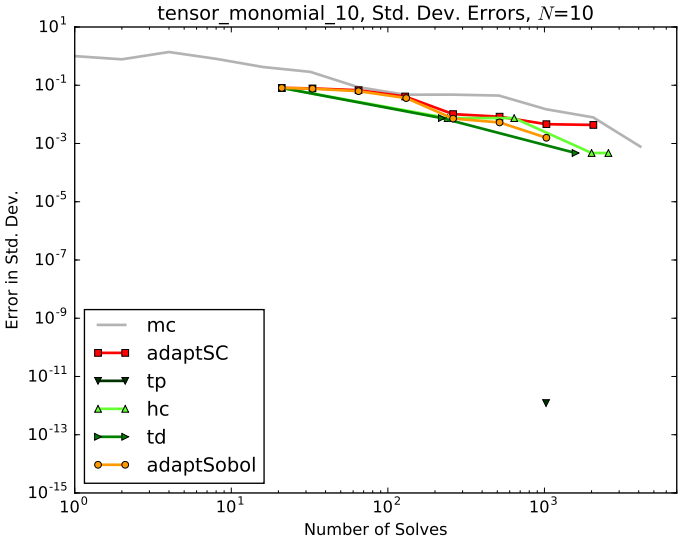

FIGURE 4.12: Tensor Monomial, $N = 10$, Std. Dev. Convergence

4.3 Sudret Polynomial

This model is described in section 2.3.

4.3.1 3 Inputs

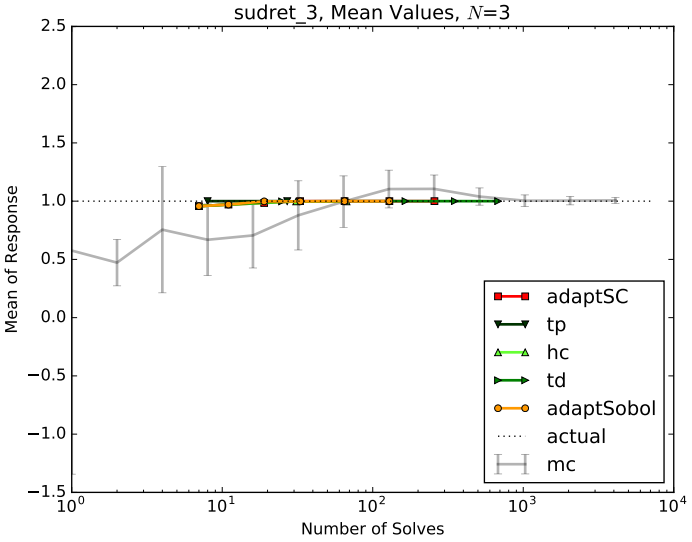

FIGURE 4.13: Sudret Polynomial, $N = 3$, Mean Values

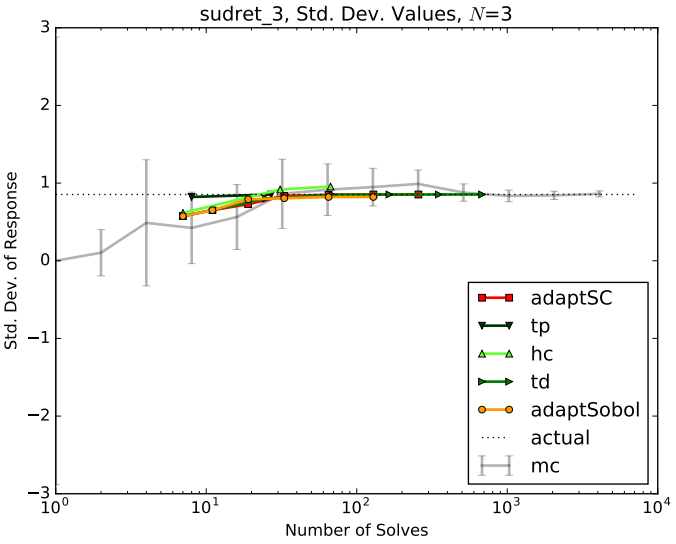

FIGURE 4.14: Sudret Polynomial, $N = 3$, Std. Dev. Values

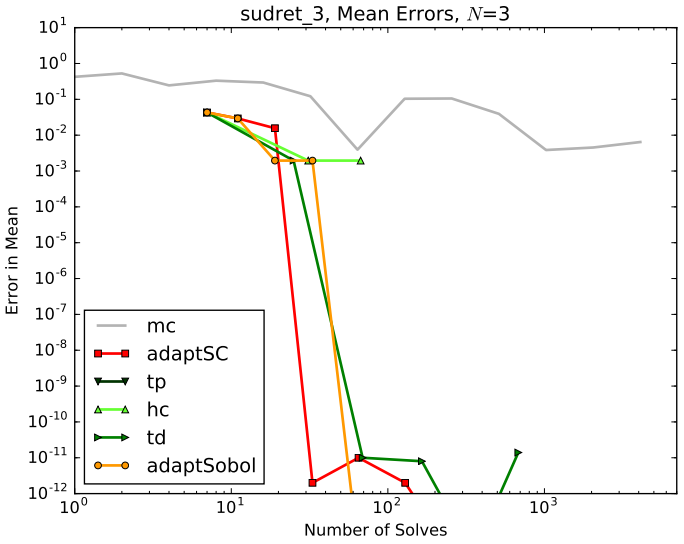

FIGURE 4.15: Sudret Polynomial, $N = 3$, Mean Convergence

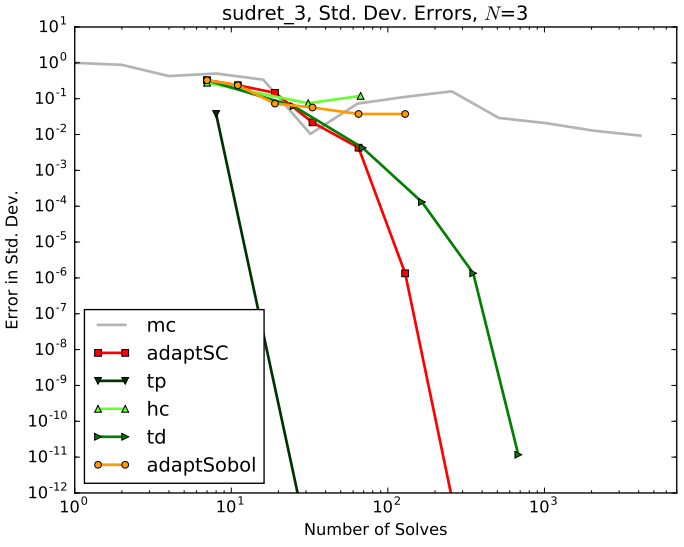

FIGURE 4.16: Sudret Polynomial, $N = 3$, Std. Dev. Convergence

4.3.2 5 Inputs

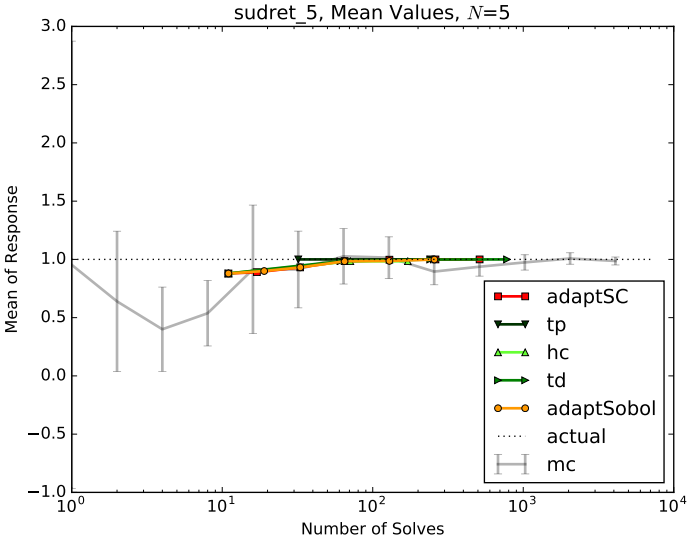

FIGURE 4.17: Sudret Polynomial, $N = 5$, Mean Values

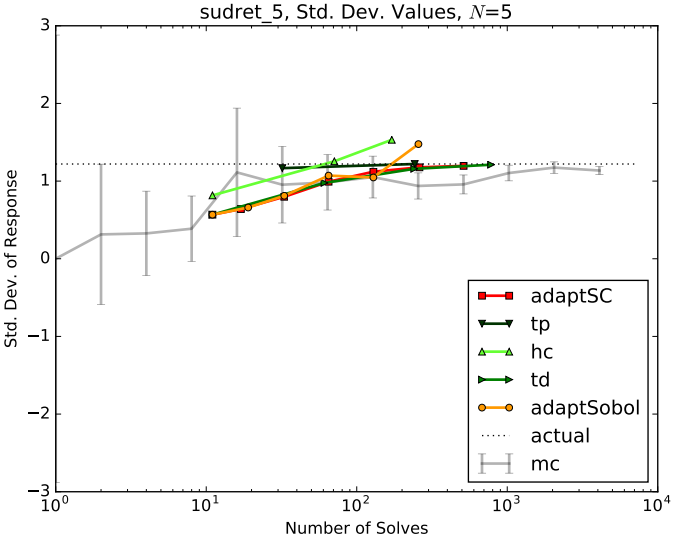

FIGURE 4.18: Sudret Polynomial, $N = 5$, Std. Dev. Values

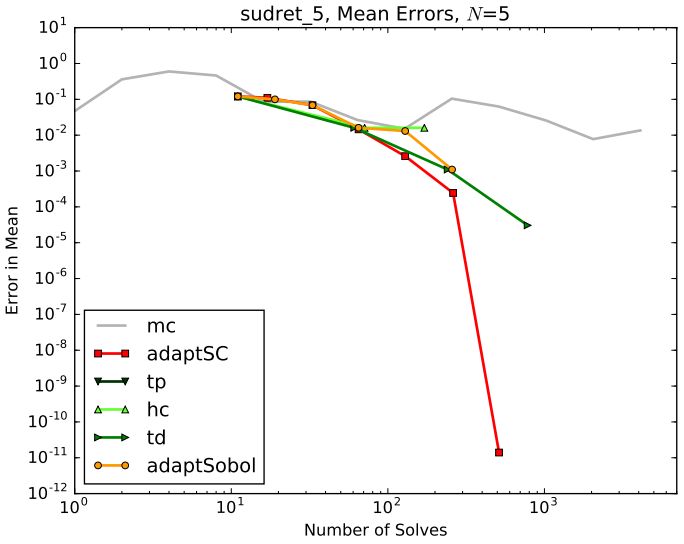

FIGURE 4.19: Sudret Polynomial, $N = 5$, Mean Convergence

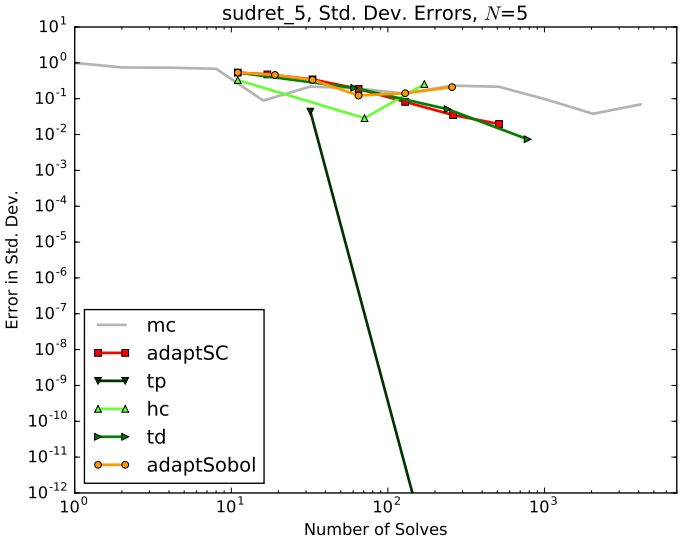

FIGURE 4.20: Sudret Polynomial, $N = 5$, Std. Dev. Convergence

4.4 Attenuation

This model is described in section 2.4.

4.4.1 2 Inputs

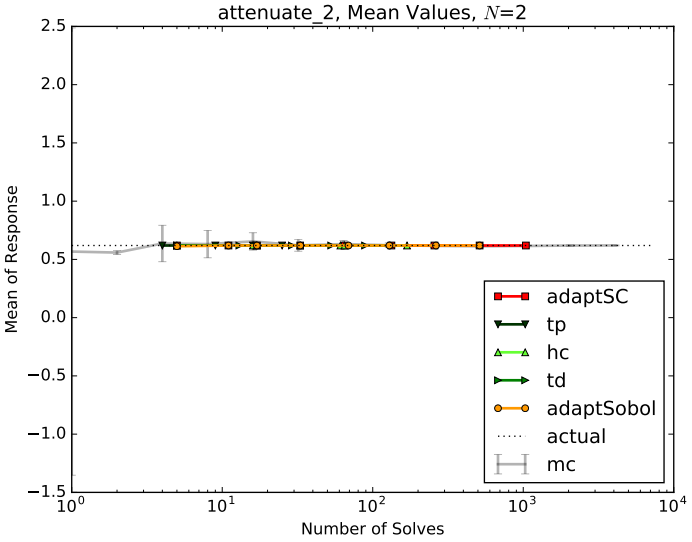

FIGURE 4.21: Attenuation, $N = 2$, Mean Values

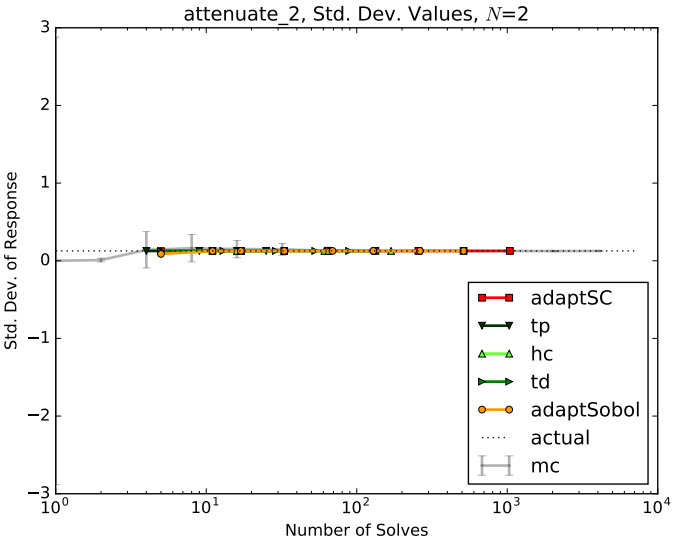

FIGURE 4.22: Attenuation, $N = 2$, Std. Dev. Values

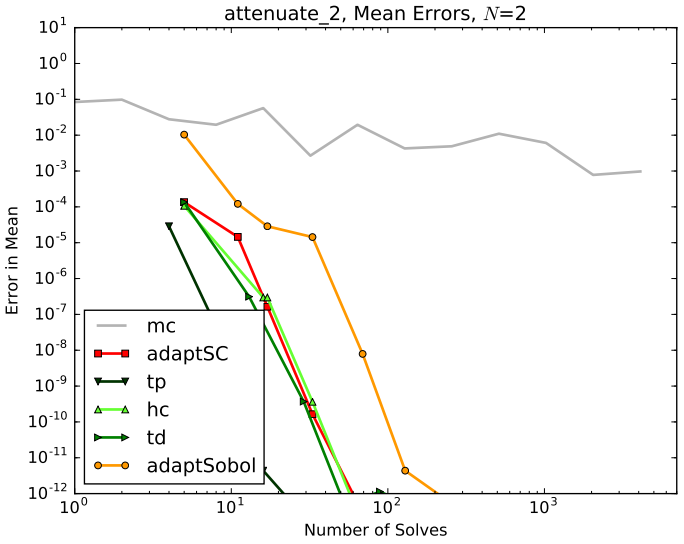

FIGURE 4.23: Attenuation, $N = 2$, Mean Convergence

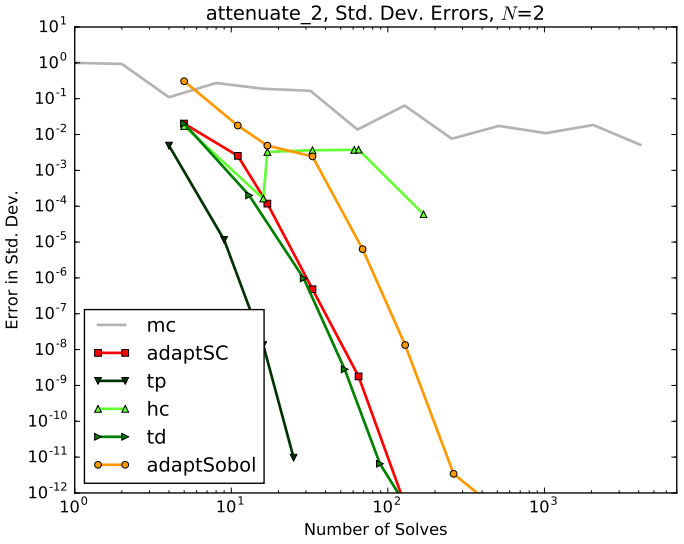

FIGURE 4.24: Attenuation, $N = 2$, Std. Dev. Convergence

4.4.2 4 Inputs

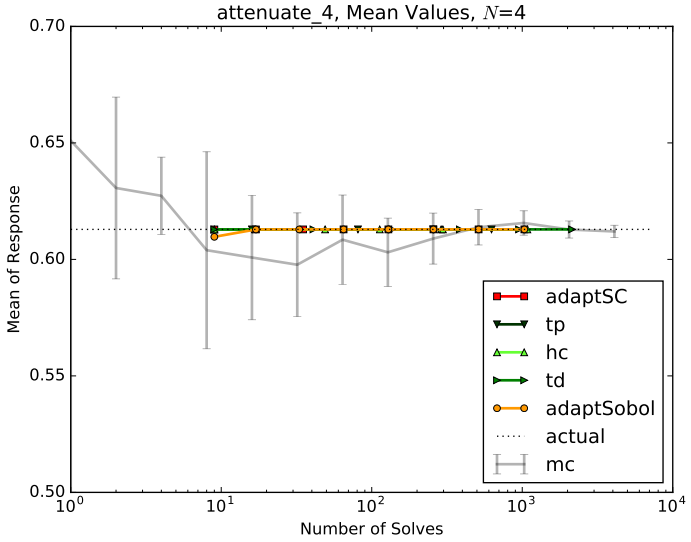

FIGURE 4.25: Attenuation, $N = 4$, Mean Values

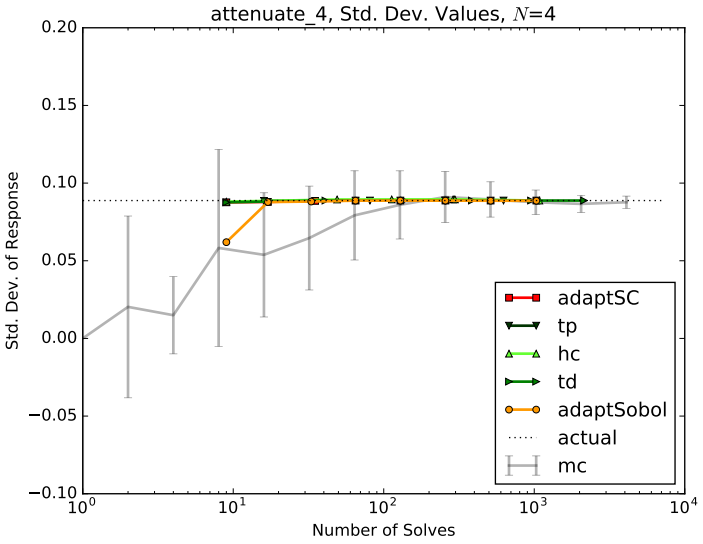

FIGURE 4.26: Attenuation, $N = 4$, Std. Dev. Values

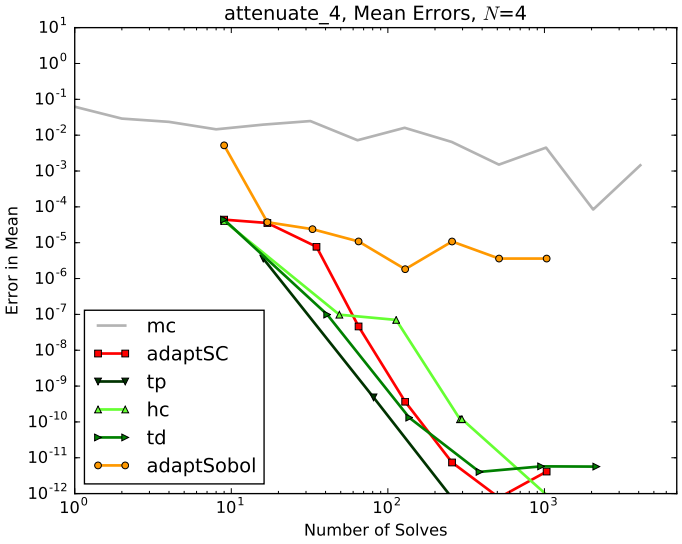

FIGURE 4.27: Attenuation, $N = 4$, Mean Convergence

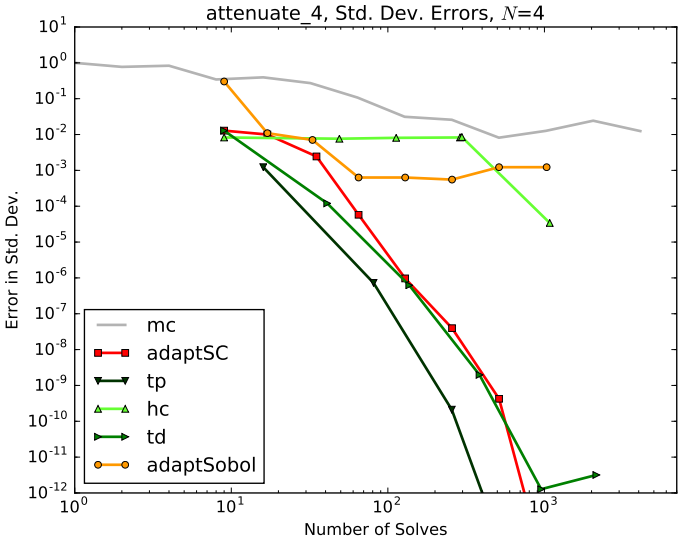

FIGURE 4.28: Attenuation, $N = 4$, Std. Dev. Convergence

4.4.3 6 Inputs

4.5 Gauss Peak

This model is described in section 2.5.

4.6 Ishigami

This model is described in section 2.6.

4.7 Sobol G-Function

This model is described in section 2.7.

4.8 Anisotropic Polynomial

This model is described in section 2.8.

Chapter 5

Engineering Demonstration

5.1 Todo

todo.

Chapter 6

Conclusions

6.1 Todo

todo.

Chapter 7

Future Work

7.1 Introduction

The results in this work lead to several interesting areas of improvement. We discuss some of these briefly here.

7.2 Impact Inertia in Adaptive Samplers

One weakness demonstrated in the adaptive sampling techniques is the phenomenon of purely-even or purely-odd polynomial representations. This is seen clearly in the Ishigami 2.6 and Gauss Peak 2.5 models. Consider the Taylor development of a sine function,

$$\sin x = x - \frac{x^3}{6} + \frac{x^5}{120} + \mathcal{O}(x^7), \tag{7.1}$$

and for a square exponential,

$$e^{-x^2} = 1 - x^2 + \frac{x^4}{2} - \frac{x^6}{6} + \frac{x^8}{24} + \mathcal{O}(x^10). \tag{7.2}$$

Unique to both of these functions is "skipping" certain polynomial orders (evens for sine, odds for square exponential).

In a single-dimension example, the current impact estimation expression is

$$\tilde{\eta_k} = \eta_{k-1}. \tag{7.3}$$

Because adaptive sampling currently relies on the previous-order polynomial to estimate the importance of the current polynomial, it can be misled into thinking there is no additional information to gather if certain polynomials are not present in the expansion.

For example, if the adaptive sampler finds the impacts of a one-dimensional problem to be 0.4 for x, it will try x^2. If the model is an odd function, it will find the impact for x^2 is actually zero. As a result, it will be very unlikely to try x^3, despite the fact that x^3 has significant real impact.

One resolution to this method is to apply some sort of *impact inertia* to the estimation of impact values; that is, in addition to considering the previous polynomial impact when estimating current polynomial impact, several previous polynomials might be considered. This kind of inertia is likely problem-dependent in its effectiveness, and would be best controlled through an optional user input. Some research would be required to determine what default level of inertia is recommended. The new impact estimation expression would be something like the following:

$$\tilde{\eta_k} = \frac{1}{\alpha} \sum_{n=1}^{k} \frac{1}{g(n)} \eta_{k-n}, \tag{7.4}$$

where α is a balancing parameter and $g(n)$ is a penalty function that grows as $k - n$ increases.

7.3 Cross-Communication in Adaptive HDMR

Todo, basically if I want the next step in (x,y), that next step shouldn't be a polynomial containing 0 in either x or y.

Bibliography

[1] Ayres and Eaton. Uncertainty quantification in nuclear criticality modelling using a high dimensional model representation. *Annals of Nuclear Energy*, 80:379–402, May 2015.

[2] Rabiti, Cogliati, Pastore, Gardner, and Alfonsi. Fuel reliability analysis using bison and raven. In *PSA 2015 Probabilistic Safety Assessment and Analysis*, Sun Valley, Idaho, April 2015.

[3] McKay, Beckman, and Conover. A comparison of three methods for selecting values of input variables in the analysis of output from a computer code, 1979.

[4] Wiener. The homogeneous chaos. *American Journal of Mathematics*, 60:897–936, 1938.

[5] Babuska, Tempone, and Zouraris. Galerkin finite element approximations of stochastic elliptic partial differential equations. *SIAM Journal on Numerical Analysis*, 42(2):800–825, 2004.

[6] Gleicher, Williamson, Ortensi, Wang, Spencer, Novascone, Hales, and Martineau. The coupling of the neutron transport application rattlesnake to the nuclear fuels performance application bison under the moose framework. Technical report, Idaho National Laboratory (INL), 2015.

[7] Gaston, Newman, Hansen, and Lebrun-Grandié. Moose: a parallel computational framework for coupled systems of nonlinear equations. *Nuclear Engineering and Design*, 239(10):1768 – 1778, 2009.

[8] Newman, Hansen, and Gaston. Three dimensional coupled simulation of thermomechanics, heat, and oxygen diffusion in nuclear fuel rods. *Journal of Nuclear Materials*, 392(1):6 – 15, 2009.

[9] Rabiti, Alfonsi, Mandelli, Cogliati, and Kinoshita. Raven, a new software for dynamic risk analysis. In *PSAM 12 Probabilistic Safety Assessment and Management*, Honolulu, Hawaii, June 2014.

[10] Wang. Nonlinear diffusion acceleration for the multigroup transport equation discretized with sn and continuous fem with rattlesnake. In *Proceedings of the International Conference on Mathematics and Computational Methods Applied to Nuclear Science & Engineering (M&C 2013)*, Sun Valley, Idaho, May 2013.

[11] Xiu and Karniadakis. The wiener–askey polynomial chaos for stochastic differential equations. *SIAM Journal on Scientific Computing*, 24(2):619–644, 2002.

[12] Askey and Wilson. Some basic hypergeometric orthogonal polynomials that generalize jacobi polynomials. *Memoirs of the American Mathematical Society*, 54:1–55, 1985.

[13] Novak and Ritter. The curse of dimension and a universal method for numerical integration. In Günther Nürnberger, JochenW. Schmidt, and Guido Walz, editors, *Multivariate approximation and splines*, volume 125 of *ISNM International Series of Numerical Mathematics*, pages 177–187. Birkhäuser Basel, 1997.

[14] Smolyak. Quadrature and interpolation formulas for tensor products of certain classes of functions. In *Dokl. Akad. Nauk SSSR*, volume 4, page 123, 1963.

[15] Trefethen. Is guass quadrature better than clenshaw-curtis? *SIAM Review*, 50(1): 67–87, 2008.

[16] Gerstner and Griebel. Dimension-adaptive tensor-product quadrature. *Computing*, 71, 2003.

[17] Boulore, Struzik, and Gaudier. Uncertainty and sensitivity analysis of the nuclear fuel thermal behavior. *Nuclear Engineering and Design*, 253:200–210, 2012.

[18] Argonne National Laboratory. Argonne code center: benchmark problem book. *ANL-7416 M&C Division of ANS*, 1968.

[19] Babuska, Nobile, and Tempone. A stochastic collocation method for elliptic partial differential equations with random input data. *SIAM Journal on Numerical Analysis*, 45, 2007.

[20] Li, Rosenthal, and Rabitz. High dimensional model representations. *J. Phys. Chem. A*, 105, 2001.

[21] Hu, Smith, Willert, and Kelley. High dimensional model representations for the neutron transport equation. *NS&E*, 177, 2014.

[22] Nobile, Tempone, and Webster. A sparse grid stochastic collocation method for partial differential equations with random input data. *SIAM Journal on Numerical Analysis*, 46, 2008.

[23] Barthelmann, Novak, and Ritter. High dimensional polynomial interpolation on sparse grids. *Advances in Computational Mathematics*, 12, 2000.

[24] Bungartz and Griebel. Sparse grids. *Acta Numerica*, 13, 2004.

[25] Le Maître and Knio. *Spectral methods for uncertainty quantification with applications to computational fluid dynamics*. Springer, 1st edition, 2010.

[26] Fichtl and Prinja. The stochastic collocation method for radiation transport in random media. *J. Quantitative Spectroscopy & Radiative Transfer*, 12, 2011.

[27] Rising, Prinja, and Talou. Prompt fission neutron spectrum uncertainty propagation using polynomial chaos expansion. *Nucl. Sci. Eng.*, 175, 2013.

[28] Talbot, Wang, Rabiti, and Prinja. Multistep input reduction for high dimensional uncertainty quantification in raven code. *Proceedings of PHYSOR*, 2016.

[29] SCALE Manual Scale ORNL. Scale: A comprehensive modeling and simulation suite for nuclear safety analysis and design. *ORNL/TM-2005/39, Version*, 6.

[30] Sudret. Global sensitivity analysis using polynomial chaos expansions. *Reliability Engineering & System Safety*, 93(7):964–979, 2008.

[31] Genz. A package for testing multiple integration subroutines. In *Numerical Integration*, pages 337–340. Springer, 1987.

[32] T Ishigami and Toshimitsu Homma. An importance quantification technique in uncertainty analysis for computer models. In *Uncertainty Modeling and Analysis, 1990. Proceedings., First International Symposium on*, pages 398–403. IEEE, 1990.

[33] Amandine Marrel, Bertrand Iooss, Beatrice Laurent, and Olivier Roustant. Calculations of sobol indices for the gaussian process metamodel. *Reliability Engineering & System Safety*, 94(3):742–751, 2009.